New calculation for the neutron-induced fission cross section of ^{233}Pa between 1.0 and 3.0 MeV

J. Mesa,[1] J. D. T. Arruda-Neto,[1,2] A. Deppman,[1] V. P. Likhachev,[1] M. V. Manso,[1,3] C. E. Garcia,[1,3] O. Rodriguez,[1,3] F. Guzmán,[3] and F. Garcia[4]

[1]*Instituto de Física, Universidade de São Paulo, São Paulo, Brazil*
[2]*Universidade de Santo Amaro/UNISA, São Paulo, Brazil*
[3]*Instituto Superior de Ciencias y Tecnologia Nucleares, Havana, Cuba*
[4]*Universidade Estadual de Santa Cruz, Ilhéus-Bahia, Brazil*

(Received 24 April 2003; published 20 November 2003)

The ^{233}Pa(n, f) cross section, a key ingredient for fast reactors and accelerators driven systems, was measured recently with relatively good accuracy [F. Tovesson *et al.*, Phys. Rev. Lett. **88**, 062502 (2002)]. The results are at strong variance with accepted evaluations and an existing indirect experiment. This circumstance led us to perform a quite detailed and complete evaluation of the ^{233}Pa(n, f) cross section between 1.0 and 3.0 MeV, where use of our newly developed routines for the parametrization of the nuclear surface and the calculation of deformation parameters and level densities (including low-energy discrete levels) were made. The results show good quantitative and excellent qualitative agreement with the experimental direct data obtained by Tovesson *et al.* [F. Tovesson *et al.*, Phys. Rev. Lett. **88**, 062502 (2002)]. Additionally, our methodology opens new possibilities for the analysis of subthreshold fission and above threshold second-chance fission for both ^{233}Pa and its decay product ^{233}U, as well as other strategically important fissionable nuclides.

DOI: 10.1103/PhysRevC.68.054608 PACS number(s): 25.85.Ec, 24.75.+i, 28.20.−v

I. INTRODUCTION: THE PROTACTINIUM EFFECT

Quite recently, Tovesson and collaborators published results from first time measurements of the neutron-induced fission cross section of ^{233}Pa at four neutron energies between 1.0 and 3.0 MeV [1]. It was observed that the results are lower than all existing theoretical predictions, as well as lower than an indirect measurement (see, in particular, Fig. 1 of Ref. [1]).

In thorium fueled nuclear systems, neutron capture by ^{232}Th leads to the formation of ^{233}Th which decays by β emission, with a half-life of ~22 min, to ^{233}Pa. Thus, the isotope ^{233}Pa is quite important in intermediating the production of the nuclear fuel ^{233}U, since the former is produced by the decay of the latter with a half-life of ~27 days, which should be compared with the ~2.4 day half-life of ^{239}Np (the intermediate isotope in the ^{238}U-^{239}Pu fuel cycle). Although not a long-lived isotope, ^{233}Pa is anyway of much concern because each neutron capture by ^{233}Pa leads to both one neutron depletion and one ^{233}U atom to be lost, which confers to the reaction ^{233}Pa(n, f) a strategical status.

The buildup and decay of ^{233}Pa, which affect both the breeding and the reactivity behavior, is referred to in literature as the "protactinium effect" [2,3]. In fact, in the case of fast breeder reactors employing thorium, the transient reactivity effects arising from the protactinium effect should, thus, be carefully evaluated and taken into account in design and operation. For example, the first one month of operation will register a substantial fall in the reactivity, as a consequence of the ^{233}Pa buildup and its delayed decay (27 day half-life) to ^{233}U. Also, to fully appreciate the role played by ^{233}Pa in the energy amplifier concept of Carlos Rubbia we refer the reader to Ref. [4].

Interestingly too, ^{233}Pa has raised weapon-proliferation concerns as discussed in the study by Bowman [5] on the accelerator driven transmutation technology project, where it is theoretically shown that a sizable fraction of the estimated inventory of ^{233}Pa could be extracted to produce pure weapon grade ^{233}U.

Therefore given the strategical importance of ^{233}Pa as an intermediary element in a ^{232}Th fueled reactor, its (n, f) cross section at fast neutron energies must be known with an accuracy better than 20%, as stated elsewhere for fast reactors and accelerator driven systems [2]. In some key applications accuracies much better than 20% are required, as, e.g., in the calculations of the ^{233}Pa reactivity effect on the shutdown margin in neutron benchmark for accelerator driven systems [6].

Our attention to the ^{233}Pa(n, f) issue was called for by the fact that published experimental data present total uncertainties in the 10% range [1], but they are at strong variance with accepted evaluations. Although experimental results have a higher status than that of calculations, such observed discrepancies cry for an elucidation, given the paramount importance of the ^{233}Pa(n, f) results and, moreover, because there is to date no other corroborating direct or indirect experiment.

We present in this paper the result of a quite detailed and complete calculation for the ^{233}Pa(n, f) cross section, highlighted by the use of state of the art routines developed by our group for the parametrization of the nuclear surface and the calculation of deformation parameters and level densities (including low-energy discrete levels).

II. CALCULATIONS

The cross section for fission induced by neutrons of energy E is given by

TABLE I. Deformation parameters obtained for the most relevant points of the fission path of ^{234}Pa. For the first three points, only the elongation and quadrupolar deformation parameters (ε and α_4, respectively) were considered. For the outer saddle point the asymmetric mass distribution of fragments is considered via the octupolar deformation parameter (α_3).

	ε	α_4	α_3
Equilibrium deformation	0.212	0.078	
First saddle point	0.400	−0.062	
Second well	0.490	0.024	
Second saddle point	0.710	0.025	0.110

$$\sigma_{nf}(E) = \frac{\lambda}{8\pi(2I_0+1)} \sum_{\ell j J^\pi} (2J+1) \cdot T_{\ell j}^{J^\pi}(E) P_f^{J^\pi}(E) \cdot S_{nf}^{\ell j J^\pi}, \tag{1}$$

where $T_{\ell j}^{J^\pi}$ and $P_f^{J^\pi}$ are the neutron penetrability and the fission probability, respectively. I_0 is the target nucleus spin, and ℓ and s are the orbital angular momentum and spin of the neutron, respectively, with $J=I_0+j$ and $j=\ell+s$. $S_{nf}^{\ell j J^\pi}$ takes into account the Porter-Thomas fluctuations of neutron, fission, and radiative widths [7].

The fission probability of a level J^π populated by neutron absorption is

$$P_f^{J^\pi}(E) = \frac{\Gamma_f^{J^\pi}(E)}{\Gamma_f^{J^\pi}(E) + \Gamma_n^{J^\pi}(E) + \Gamma_\gamma^{J^\pi}(E)}, \tag{2}$$

where $\Gamma_f^{J^\pi}$, $\Gamma_n^{J^\pi}$, and $\Gamma_\gamma^{J^\pi}(E)$, the fission, neutron, and gamma widths, are obtained for the corresponding transmission coefficients, T_f, T_n, and $T_\gamma^{X\ell}$, and level densities.

A. γ channel

γ ray transmission coefficients are related to the well known γ strength functions $f_\gamma^{X\ell}(E_\gamma)$ with multipolarities $X\ell$ (X denotes the electric or magnetic character of the transition) by

$$T_\gamma^{X\ell}(E_\gamma) = 2\pi E_\gamma^{2\ell+1} f_\gamma^{X\ell}(E_\gamma), \tag{3}$$

where E_γ is the γ ray energy.

We obtained $f_\gamma^{X\ell}$ from the Brink-Axel approximation (as reviewed in Ref. [8]), where the photoabsorption cross section for $E1$ was represented by a Lorentzian shaped giant dipole resonance with parameters obtained by interpolation of those from ^{232}Th and ^{238}U [9], which are quite similar to each other. For f_γ^{E2} and f_γ^{M1} we used the Weisskopf approximation [10], which works reasonably well for actinides near the fission threshold, as discussed by us elsewhere [11].

It should be noted, notwithstanding, that $E1$ transitions in actinides dominate the low energy region near the fission threshold. Anyway, the whole contribution of Γ_γ to the fission probability is small and structureless, in comparison to Γ_f and Γ_n.

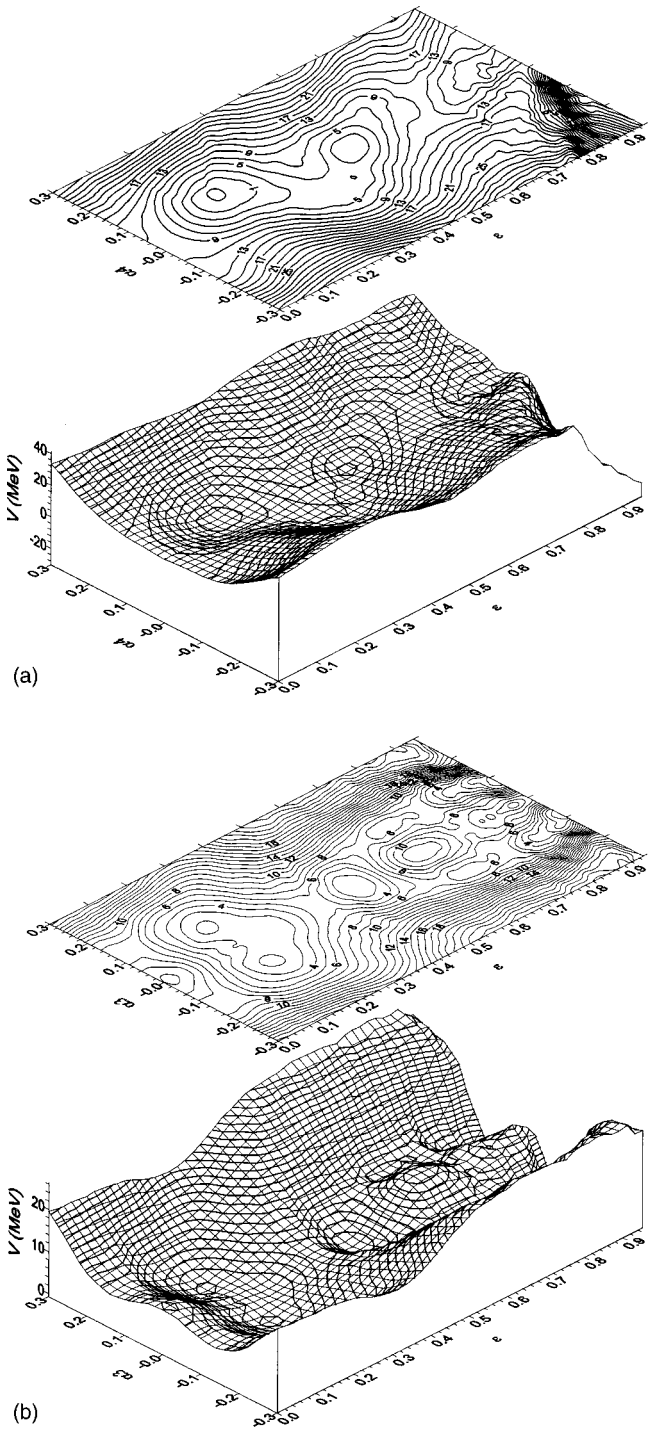

FIG. 1. Calculated potential energy topography of ^{234}Pa (bottom) and the corresponding equipotentials (top), as a function of the deformation parameters ε and α_4 (a) and ε and α_3 (b).

B. Neutron channel

The neutron transmission coefficients are given by

$$T_n(E) = \sum_{\ell j d} T_{\ell j}^{J^\pi}(E^* - E_d) + \sum_{\ell j d} \int_0^{E^*-E_c} T_{\ell j}^{J^\pi}(\widetilde{E}) \rho(E^* - \widetilde{E}, I, \pi) d\widetilde{E}, \tag{4}$$

where $E^*=E+B_n$ is the excitation energy, and E_d is the

TABLE II. Fission barrier parameters used as input in our calculations.

	B_A (MeV)	$\hbar\omega_A$ (MeV)	Symmetry	B_B (MeV)	$\hbar\omega_B$ (MeV)	Symmetry
^{234}Pa	6.30	0.60	Axial	6.15	0.40	Axial-mass asymmetric

energy of a discrete level in the residual nucleus (^{233}Pa). Also, $T_{\ell j}^{J^\pi}$ is the neutron transmission coefficient in the entrance channel, ρ is the level density of the residual nucleus at the equilibrium deformation, and E_c is the cutoff energy.

The emitted neutron transmission coefficients were calculated using the same deformed optical potential as that for the neutron entrance channel, the latter being calculated through the coupled channels approach, with potential parameters obtained from those of the systematic of actinide deformed optical potential [12].

C. Fission channel

When considering a double-humped fission barrier, and an excitation energy higher than both barrier humps, fission is viewed as a two-step process, namely, the successive crossing over of the inner (A) and the outer (B) humps. In this case, the levels and level density in the inner and outer humps are used to calculate the transmission coefficients.

The height of fission barriers obtained by theoretical calculations is very sensitive to the adopted model parameters [13]. Although we had estimated the total fission barrier with our formalism, we preferred to adopt the recommended fission barrier height and curvatures [14]—see Table I. We considered only the deformation parameters obtained from fission path deduced from the variational principle [13] (for saddle points, because for the equilibrium deformation the parameters are rather obvious).

The transmission coefficient of the fission barrier i is defined as

$$T_{fi}^{J^\pi}(E^*) = \sum_{K=-J}^{J} T_{fi}^{J^\pi,K}(E^*) + \int_0^\infty \frac{\rho_{fi}(\varepsilon, J, \pi)}{\left\{1+\exp\left[\frac{2\pi}{\hbar\omega_i}(E_{fi}+\varepsilon-E^*)\right]\right\}}\, d\varepsilon, \quad (5)$$

where E_{fi} and $\hbar\omega_i$ are the height and the curvature of barrie i (i=A or B), respectively, and ρ_{fi} is the level density at the corresponding saddle point. The first term at the right-hand side of Eq. (5) corresponds to contributions of low-lying discrete collective states obtained from the calculated quasiparticle and rotational spectra up to ~600 keV at saddle point deformations. It is exactly expressed if we consider an inverted parabolic barrier [13]. The second term accounts for the continuum of levels associated with a given saddle deformation. ε is the intrinsic excitation energy of the fissioning nucleus.

Therefore, the transmission coefficient of the fission channel is given by

$$T_f^{J^\pi}(E^*) = \frac{T_{fA}^{J^\pi}(E^*)\,T_{fB}^{J^\pi}(E^*)}{T_{fA}^{J^\pi}(E^*)+T_{fB}^{J^\pi}(E^*)}. \quad (6)$$

The widths Γ_γ, Γ_n, and Γ_f are obtained from the corresponding transmission coefficients (see above) plus the level densities appropriate to each situation, namely, (a) γ channel, levels of the compound nucleus ^{234}Pa* at the equilibrium deformation; (b) neutron channel, levels of the residual nucleus ^{233}Pa* at the equilibrium deformation; and (c) fission channel, levels of the compound nucleus ^{234}Pa* at the saddle points deformations.

The starting point to calculate all these level densities is to obtain the set of nuclear deformation parameters at both the equilibrium and saddle points. This is achieved from our code BARRIER [15], where the complete mapping of the nuclear potential energy $V(\varepsilon, \alpha_4)$ is obtained as a function of the deformation parameters ε and α_4, which are related to the elongation and hexadecapolar momenta, respectively [15]—see Fig. 1 and Table II. The nuclear shapes associated with each point $V(\varepsilon, \alpha_4)$ of the fission path were obtained by means of Cassinian ovals parametrization, in order to have a better calculation of the single-particle orbitals, even at extreme deformations (including the two-center problem) [16]; the results are shown in Fig. 2. For the outer saddle point B we also took into account the octupolar deformation α_3 in order to describe the mass asymmetry of the fission fragments.

D. Level densities

The deformation parameters at minima and maxima of the fission path (see in Table II the output of our code BARRIER

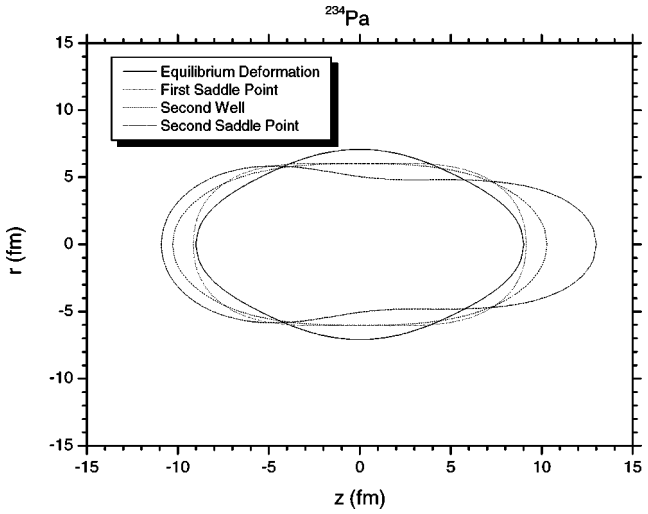

FIG. 2. Calculated nuclear shapes associated with the most relevant points of $V(\varepsilon, \alpha)$ along the fission path (this work).

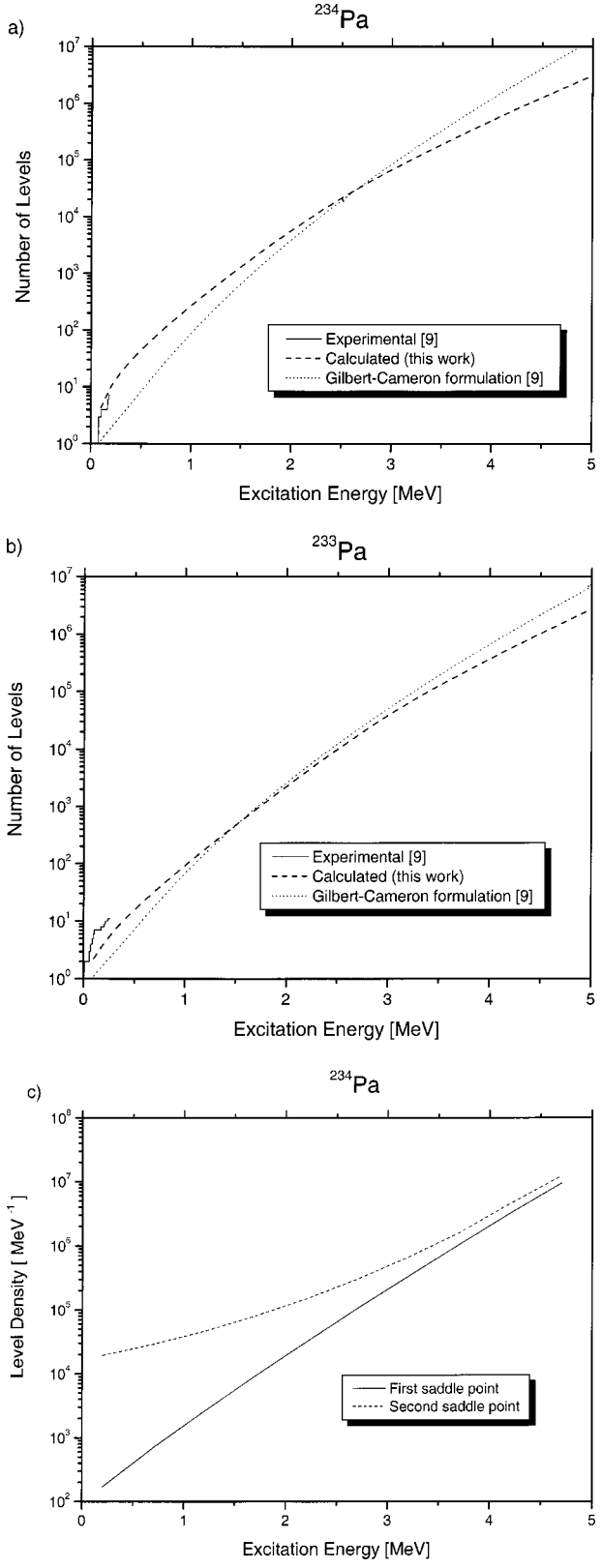

FIG. 3. Calculated (this work) and experimental numbers of cumulative levels for ^{234}Pa (a) and ^{233}Pa (b). Calculated total level densities in the first and the second saddle point (c).

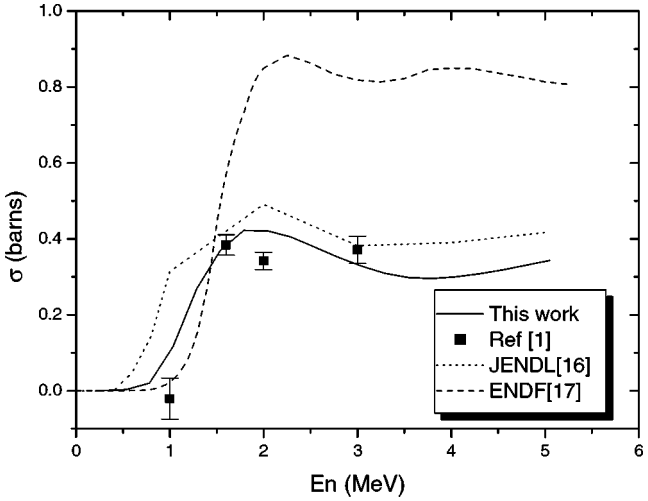

FIG. 4. Neutron-induced fission cross section of ^{233}Pa measured by Tovesson *et al.* (data points Refs. [1]) and the result of our calculation (full curve). Also shown are two previous evaluations (Refs. [16,17]).

[15]), and the corresponding calculated single-particle orbitals, were used as input in the calculation of quasiparticle and rotational spectra. In this sense, a more realistic level density calculation was performed, using a semimicroscopical method with the Lipkin-Nogami projectors in the BCS approach [17]. For the continuum in the adiabatic approximation, the total level density can be factorized as

$$\rho(E^*, J^\pi) = K_{rot}(E^*, J^\pi) K_{vib}(E^*) \rho_{qp}(E^*, J^\pi), \qquad (7)$$

where $\rho_{qp}(E^*, J^\pi)$ is the density of quasiparticle levels, while K_{rot} and K_{vib} are the rotational and vibrational enhancement factors of the level density, respectively [18].

We refer the reader to Ref. [13] for the description of the usual way to calculate K_{rot}.

For the calculation of K_{vib} we used the nonadiabatic formalism for a single deformation parameter proposed by Diaz-Torres *et al.* [19], which we adapted for the more general case of multiple deformation parameters [20].

The quasiparticle level density ρ_{qp} was calculated from the quantum-statistical superfluid model in the framework of the approach we have recently developed [17]. The calculated cumulative number of levels for ^{234}Pa (compound nucleus) and ^{233}Pa (residual nucleus) are shown in Figs. 3(a) and 3(b). It is important to note that the Gilbert Cameron formula [14], adopted in nearly all evaluations, always underestimates the cumulative number of levels. With our calculations the experimental [14] cumulative number of levels of ^{234}Pa is reproduced with success, while for ^{233}Pa we have a better result in comparison to that from the Gilbert-Cameron formulation. For saddle point configurations, the corresponding level densities calculated with our model are shown in Fig. 3(c).

III. RESULTS AND DISCUSSION

The final result of our $\sigma_{n,f}$ calculation is shown in Fig. 4, together with the experimental results from Tovesson *et al.*

[1] and evaluations from JENDL [21] and ENDF/B-VI [22]. Good quantitative agreement is achieved between experiment and our results in the whole 1−3 MeV energy range, while the trend of the experimental data, in particular, is nicely reproduced.

The ENDF/B-VI evaluation, on one hand, describes well the near-threshold points but greatly overestimates higher energy points. On the other hand, the JENDL evaluation has a better performance above ~1.5 MeV, but fails badly near the threshold.

After comparing our methodology with those used in the above mentioned evaluations, we make salient the following distinct ingredients present in it: (1) the nuclear shape parametrization in terms of Cassinian ovals [15,16] and (2) more realistic level density calculations using the Lipkin-Nogami projectors in the BCS approach [17].

Additionally, while in the JENDL and ENDF/B-VI evaluations use was made of extensive and continuous level density expressions, in our calculations we used a discrete set of calculated levels up to $E \sim 600$ keV at the saddle point deformations. This could partially explain the better performance of our calculations. Also, by employing more realistic and precise calculations we could use recommended fission barrier parameters (Table I) directly, without the need of pushing them up or down as adjustable parameters.

It is anticipated in Ref. [1] that there is a possibility of performing in the future more ^{233}Pa(n, f) measurements with emphasis on the threshold regions for both prompt and second-chance fission processes. This would allow for better determination of the thresholds themselves, which are crucial inputs for full and precise calculations. In this sense, it would be possible to take advantage of our more sophisticated methodology in order to obtain information also from the subthreshold fission process, while extending the data analysis beyond second-chance fission. In the meantime, we will turn our attention to other (n, f) reactions, e.g., ^{233}U(n, f), which plays an important role in the determination of the ^{233}Pa(n, f) experimental yield (^{233}U is a decay product of ^{233}Pa).

ACKNOWLEDGMENTS

This work was partially supported by FAPESP and CNPq, Brazilian agencies, and CLAF (Latinamerican Center for Physics).

[1] F. Tovesson, F.-J. Hambsch, A. Oberstedt, B. Fogelberg, E. Ramstrom, and S. Oberstedt, Phys. Rev. Lett. **88**, 062502 (2002).
[2] V. G. Pronyaev, IAEA Report No. INDC(NDS)-408, 1999.
[3] S. Ganesan, in *Proceedings of the International Topical Meeting on Advances in Reactor Physics and Mathematics and Computation into the Next Millennium* (American Nuclear Society, Pittsburgh, PA, 2000).
[4] C. Rubbia *et al.*, CERN Group, Report IAEA-TECDOC-985, International Atomic Energy Status Report, 1997, pp. 187–312.
[5] C. Bowman, Report IAEA-TECDOC-985, International Atomic Energy Status Report, 1997, pp. 135–153.
[6] S. Pelloni, G. Youinou, and P. Wydler, in *Proceedings, of the International Conference on Nuclear data for Science and Technology, Trieste, 1997*, edited by G. Reffo, A. Ventura, and C. Grandi (Italian Physical Society, Bologna, Italy, 1997), Vol. 59, Part II, pp. 1172–1176.
[7] C. E. Porter and R. G. Thomas, Phys. Rev. **104**, 483 (1956).
[8] E. Betak, F. Cvelbar, A. Likar, and T. Vidmar, Nucl. Phys. **A686**, 204 (2001).
[9] B. L. Berman, J. T. Cadwell, E. J. Dowdy, S. S. Dietrich, P. Meyer, and R. A. Alvarez, Phys. Rev. C **34**, 2201 (1986).
[10] J. M. Blatt and V. F. Weisskopf, *Theoretical Nuclear Physics* (Wiley, New York, 1952), p. 627.
[11] J. D. T. Arruda-Neto, Phys. Rev. C **37**, 1326 (1988).
[12] G. Vladuca, A. Tudora, and M. Sin, Rom. J. Phys. **41**, 515 (1996).
[13] S. Bjornholm and J. E. Lynn, Rev. Mod. Phys. **52**, 725 (1980).
[14] Reference Input Parameter Library, Report No. IAEA-Tecdoc-1034, 1998 (also available at http://iaeand.iaea.or.at/ripl).
[15] F. Garcia, O. Rodriguez, J. Mesa, J. D. T. Arruda-Neto, V. P. Likhachev, E. Garrote, R. Capote, and F. Guzmán, Comput. Phys. Commun. **120**, 57 (1999).
[16] F. Garcia, E. Garrote, M.-L. Yoneama, J. D. T. Arruda-Neto, J. Mesa, F. Bringas, J. F. Dias, V. P. Likhachev, O. Rodriguez, and F. Guzman, Eur. Phys. J. A **6**, 49 (1999).
[17] O. Rodriguez, F. Garcia, H. Dias, J. Mesa, J. D. T. Arruda-Neto, E. Garrote, and F. Guzman, Comput. Phys. Commun. **137**, 405 (2001).
[18] F. Garcia, O. Rodriguez, E. Garrote, and E. Lopez, J. Phys. G **19**, 2157 (1993).
[19] A. Diaz-Torres, F. Guzman-Martinez, and R. Rodriguez-Guzman, Z. Phys. A: Hadrons Nucl. **354**, 409 (1996).
[20] J. Mesa, J. D. T. Arruda-Neto, C. E. Garcia, V. P. Likhachev, and A. Deppman (unpublished).
[21] T. Nakagawa *et al.*, J. Nucl. Sci. Technol. **32**, 1259 (1995).
[22] Cross Section Evaluation Working Group, Brookhaven National Laboratory Report No. BNL-NCS-17541 (ENDF-201), 1991.